The Cryosphere Discussions

Spatial and temporal variability in summer snow pack in the Dronning Maud Land, Antarctica

T. Vihma[1], O.-P. Mattila[2,*], R. Pirazzini[1], and M. M. Johansson[1]

[1]Finnish Meteorological Institute, P.O. Box 503, 00101 Helsinki, Finland
[2]Department of Physics, University of Helsinki, P.O. Box 64, 00014 Helsinki, Finland
[*]now at: Finnish Environmental Institute, P.O. Box 140, 00251 Helsinki, Finland

Title Page

Abstract	Introduction
Conclusions	References
Tables	Figures

|◄◄ | ►►|
|◄ | ►|

| Back | Close |

Full Screen / Esc

Printer-friendly Version

Interactive Discussion

Abstract

Snow temperature, density, and layering were measured in four summers in the Dronning Maud Land, Antarctica. Data from a 310-km-long transect showed that the most homogeneous snow pack located in the Riiser-Larsen Ice Shelf, while horizontal gradients in snow density, temperature, and hardness were larger in the escarpment region. In the local scale, day-to-day temporal variability dominated the standard deviation of snow temperature, while the diurnal cycle was next important, and horizontal variability in the scale of 0.4 to 10 m was the smallest component. The day-to-day and total small-scale variability decreased exponentially with depth with an e-folding depth at 0.25 to 0.30 m. Snow temperature depended on the cloud cover in the uppermost 0.30 m and snow density in the uppermost 0.10 m. Both in the intra-pit and transect scales, the ratio of horizontal to temporal variability increased with depth. In the intra-pit scale the temporal variability in snow density exceeded the horizontal variability throughout the uppermost 0.50 m layer, but in the 100-km scale only in the uppermost centimetres. The horizontal standard deviation of snow density increased rapidly between the scales of 0.4 and 2 m, and much more gradually from 10^1 to 10^2 m.

1 Introduction

Even in summer, more than 90% of Antarctica is covered by snow. Physical properties of snow have a strong influence on the reflection and absorption of solar radiation and the atmosphere-snow heat exchange. Antarctic snow cover is to a large extent wind packed with a small grain size, mainly due to the katabatic winds. On the coastal margin of the Antarctic continent, the wind field is also strongly affected by low-pressure systems, and horizontal gradients in precipitation, air temperature, and air humidity are large (King and Turner, 1997). Within the coastal zone, however, the mesoscale horizontal gradients may differ between the homogeneous ice shelves and escarpment regions. Some snow melt takes place in the coastal zone in summer affecting the snow pack properties while remaining unimportant for the mass balance of the whole ice sheet.

The horizontal heterogeneity in the snow pack is primarily introduced by the underlying topography, which influences the distribution of accumulation, and by the prevailing meteorological conditions, through mechanical stress by wind and melting due to radiation and air-snow heat flux (Colbeck, 1991). Sturm and Benson (2004) studied the variability of perennial and seasonal snow in Alaska, Antarctica, and Greenland in scales ranging from 10 m to 100 km. They found that the heterogeneity approaches a peak value at a scale of 100 m, and considered it to be related to wind-drift structures of approximately this size. At larger scales of tens to hundreds of kilometres synoptic-scale variations in weather forcing generate gradual variations in the characteristics of the snow pack. Although perennial snow covers are typically lying on gently varying topography, even slight topographic variations interacting with the weather often generate horizontal heterogeneity in the snow pack (Frezzotti et al., 2002a,b).

Considering vertical heterogeneity, the layering of snow pack is developed in metamorphic processes inside the snow pack driven by thermo-mechanical processes, such as heat and mass transport by the flow of water vapor and meltwater as well as densification through volumetric creep (Harper and Bradford, 2003). The layering also affects the secondary processes by directing and blocking the flow of water vapor and melt water and by altering the thermal conductivity (Colbeck, 1991). Layers formed during windy conditions are likely to be more spatially variable than other layers (Kronholm et al., 2004).

In and nearby the Dronning Maud Land, Antarctica, the region of our study, Kärkäs et al. (2002) have found large spatial variations in the snow-pack properties, and divided the study region into five principal snow zones: (1) sea ice, (2) the seaward-edge zone of the ice shelf, (3) the inner parts of the ice shelf, (4) the region above the grounding line, and (5) the local topographic highs. In addition to local topography, the distance from the coast and moisture source affects the snow properties. Kärkäs et al. (2005) observed that the annual mean values of snow grain size, conductivity, and concentrations of several inorganic chemical components decreased exponentially with increasing distance from the ice shelf edge.

Title Page

Abstract	Introduction
Conclusions	References
Tables	Figures

|◀ ▶|

◀ ▶

| Back | Close |

Full Screen / Esc

Printer-friendly Version

Interactive Discussion

Temporal variability in the snow properties is related to diurnal, synoptic-scale and seasonal changes in weather, above all the solar radiation, air temperature, precipitation, and wind speed. In the annual scale, snow density and hardness increase in summer due to thermally-driven metamorphosis and melt. In cold regions where these processes are absent or weak, seasonal variations in precipitation and wind speed may, however, dominate with larger density and hardness in winter under stronger winds and less precipitation (e.g., Meløysund et al., 2007). Granskog et al. (2006) demonstrated the strong effects of synoptic-scale variations on snow on sea ice in the Baltic Sea. Nicolaus et al. (2009) studied the diurnal cycle in snow properties in the Antarctic sea ice zone and Cheng et al. (2008a,b) in snow temperatures in the Arctic sea ice zone. Pirazzini (2004) summarized the effects of diurnal cycle of snow metamorphosis on the surface albedo in Antarctica. The diurnal temperature cycle also affects the air-snow exchange of chemical components (Frey et al., 2009).

Quantitative information on spatial and temporal variations in the snow pack is important for several reasons. Above all, measurements in snow-covered regions are usually sparse, in particular in the Antarctic and Arctic, and conclusions on the representativeness of point measurements require knowledge on the typical spatial variability in the study region. Hence, information on the spatial and temporal variability in the snow pack is essential for validation of glaciological models (Dadic et al., 2008). Combined analyses on the air-mass trajectories and large-scale spatial variability in snow are essential for interpretation of ice core results (Reijmer et al., 2002). Interpretation of climatological trends in Antarctic precipitation and the snow mass budget is sensitive to various error sources (Tietäväinen and Vihma, 2008); the spatial variability of the surface mass budget on the kilometer scale is often an order of magnitude larger than its temporal variability on the centennial time scale (Frezzotti et al., 2004). The variability in snow thickness, density, temperature, and stratigraphy is important for studies of snow surface energy and mass balance (Nicolaus et al., 2009). Further information on density variations and layering is important for interpretation of remote sensing data

(Colbeck, 1991; Kärkäs et al., 2002; Mäkynen et al., 2007), which requires ground-truth data over different spatial scales.

The above calls for more observations on spatial and temporal variability in the snow pack. To respond to this need, we have carried out snow measurements in the coastal zone of the Dronning Maud Land, Antarctica, during four austral summers. We analyse the spatial variability of snow temperature, density and layering in five different scales: <1 m, 10–20 m, 100 m, 50 km, and 100–300 km. We analyse the temporal variability in the diurnal, synoptic, and inter-annual scales, with additional focus to the effects of clouds. Our study has the following objectives:

1. to quantify the spatial variability in snow temperature, density and layering in a coastal region with a gently sloping topography but relatively large gradients (compared to inland conditions) in synoptic-scale weather conditions,

2. to better understand the relative importance of the spatial and temporal variability in snow temperature, density, and layering,

3. to obtain a better understanding of representativeness of point measurements and a better basis for planning of future field campaigns.

2 Study area and its climate

The study area, displayed in Fig. 1, covers a coastal region of the Antarctic ice sheet. In the north, the research area includes the Riiser-Larsen ice shelf. At the grounding line the ice shelf has a long peninsula here referred to as Näsen. From the grounding line the ice sheet raises gently towards the first two nunataks of the Vestfjella mountain range, Basen and Plogen. The Finnish research station Aboa is situated on the Basen nunatak. South-west from these nunataks there is the large ice rise of Högisen, with an altitude of 900 m a.s.l. The ice sheet rises gently towards southeast until it reaches a small separate rock outcrop, Fossilryggen, where the slope of the ice sheet becomes steeper. South of Fossilryggen opens the Ritchersflya ice sheet which is bounded in

Title Page

Abstract | Introduction

Conclusions | References

Tables | Figures

|◄ | ►|

◄ | ►

Back | Close

Full Screen / Esc

Printer-friendly Version

Interactive Discussion

the south by Heimefrontfjella mountain range that restrains the ice mass of the main Antarctic ice sheet.

Snow pit measurements were taken with 5 km intervals at 62 sites along the 310 km transect which starts from the edge of the Riiser-Larsen ice shelf and ends at Heimefrontfjella mountain range, 200 km inland from the grounding line (Fig. 1). The measurement site nearby Basen was located 1.5 km southwest of the nunatak. At the Aboa station on the slope of the nunatak, the local topography strongly affects the wind direction (Launiainen et al., 1995), and this effect is to a lesser extent felt also at the snow measurement site, seen as the dominating orientation of sastrugi towards northeast. In summer, parts of the nunatak surface become snow-free and are strongly heated by the solar radiation (Kärkäs, 2004), but the thermal effects are not felt at the snow measurement site.

The climate of the study region significantly varies with the distance from the coast. The effect of the transient cyclones that travel eastward along the coast decreases towards inland, whereas the effect of katabatic winds is strongest over the steepest slopes. On the basis of previous observations (van den Broeke et al., 1999, 2004; Reijmer and Oerlemans, 2002; Reijmer and van den Broeke, 2003), our study region can be divided into two climatic zones: the ice shelf (flat area along the coast) and the sloping escarpment region (consisting of Escarpment 1 between Based and Fossilryggen, and Escarpment 2 between Fossilryggen and Svea, see Fig. 1). The surface radiation budget over the whole study area is negative for most of the year and slightly positive during summer (van den Broeke et al., 2004). During winter the surface radiative loss is larger over the sloping surfaces of the escarpment region than on the flat coastal area (van den Broeke et al., 2004). The winter radiative loss is mostly compensated by the sensible heat flux from the air to the surface (Reijmer and Oerlemans, 2002). Due to the strength of the wintertime katabatic flow over the sloping areas, the annual mean wind speed is about $1.5\,\mathrm{m\,s^{-1}}$ stronger in the escarpment region near the Basen nunatak and at Svea station than over the coastal ice shelf (Reijmer and Oerlemans, 2002).

Reijmer and van den Broeke (2003) showed that in the four years 1998–2001 the annual mean snow accumulation near Basen (177±36 mm water equivalent in year – w.e. y^{-1}) was about half the snow accumulation recorded 80 km to the north over the coastal ice shelf (375±59 mm w.e. y^{-1}). Although the year-to-year variability in snow accumulation is large, the decrease in snow accumulation with increasing distance form the ice shelf edge was confirmed by Kärkäs et al. (2005) who derived yearly accumulation from δ^{18}O profiles measured during three summers.

The latitudinal gradient in near-surface air temperature, wind speed, and accumulation determines a corresponding gradient in the firn density of the uppermost metres of the snowpack. Van den Broeke et al. (1999) analysed the firn density from shallow firn cores drilled during a coastal-inland traverse in an area located slightly to the east of our study region. They observed a general decrease of the average firn density of the uppermost 1 m of snow with increasing distance from the coast, with the exception of a maximum density in correspondence of an area of topographically driven low accumulation and strong wind erosion.

3 Observations and methods

3.1 Methods

Two different methods were used to determine the snow density. Except on the traverse, in all other pits the vertical snow density profiles were measured with a steel cylinder, with a length of 0.12 m and a diameter of 0.05 m, pushed horizontally in the snow pit wall. In addition, a small aluminium box, with a height of 0.02 m, was used to sample the surface density at the same locations where the cylinder was used. The traverse was sampled using a snow fork (Sihvola and Tiuri, 1986). The dielectric method of deriving the density with the snow fork was validated in a few deeper snow pits, using the cylinder and the small density sampling box. Figure 2 shows density profiles from a single 1 m snow pit, which was measured with the snow fork, the cylinder, and

Title Page

Abstract | Introduction

Conclusions | References

Tables | Figures

|◄ | ►|

◄ | ►

Back | Close

Full Screen / Esc

Printer-friendly Version

Interactive Discussion

the small density box. The samples taken with the box were melted and density was calculated from the measure of the volume of water. The comparison of snow fork measurements against cylinder measurements showed a good agreement. The measurement method with melted samples had a bias, which is apparent from Fig. 2, but it illustrates the ability of the snow fork to capture small-scale vertical changes.

The snow temperature was measured with three types of handheld temperature probes, all having accuracy of $\pm 0.2\,°C$: Testo 4110, with a 0.30 m probe, Ebro TFX 392, with a 0.15 m probe and Ebro TLC1598, with a 0.15 m probe. The traditional subjective hardness test for snow (Colbeck et al., 1990) was used to make observations of the vertical structure of layering in the snow. Layering was determined with 0.01 m resolution. In the following, the classes of the hand test are coded as shown in Table 1.

3.2 Measurements near Basen nunatak in 2007–2008

Snow measurements nearby the Basen nunatak were made from 5 to 29 January 2007 and from 23 December 2007 to 28 January 2008. A new snow pit was excavated for each set of vertical temperature and density profiles. The following measurements were made:

(a) Snow temperature profiles at snow pits. The temperature was measured by inserting the probe horizontally into the snow at the depths of 0, 0.025, 0.05, 0.10, 0.15, 0.20, 0.25, 0.30, 0.40, and 0.50 m. The probe was also pushed downward from the bottom of the snow pit, to reach the depth of 0.90 m. At each snow pit one to three (on average 2.3) profiles with approximately 0.4 m horizontal intervals were measured. These measurements were made once or twice a day. It was difficult to push the 0.30-m-long probe exactly horizontally to the snow pack, and the accuracy of the measurement depth was studied in the field. In January 2007, a systematic error of 0.02–0.06 m, increasing with depth, was detected, and a correction was applied to the depth data. In December 2007–January 2008, no systematic error was found. During the 2006–2007 (2007–2008) campaign, 45 (32) snow pits were measured in 24 (19) days.

(b) Horizontal profiles of snow temperature. The temperature was measured along a 10–20 m long line, with 1 m intervals, manually pushing the probe vertically at the depths of 0, 0.025, 0.05, 0.10, 0.15, 0.20, and 0.275 m. Altogether 18 profiles were measured.

(c) Snow density measurements at snow pits. The density was measured with the density cylinder at the depths of 0.10, 0.20, 0.30, 0.40, and 0.50 m, and at the surface using the small density box. The samples were not melted but weighted. At each snow pit one or two density profiles, with approximately 0.4 m horizontal interval, were measured. These measurements were made at new snow pits once or twice a day. During the 2006–2007 (2007–2008) campaign, density measurements were made in 37 (27) snow pits in 24 (19) days.

(d) Horizontal profiles of snow density. The measurements were made along a 10–20 m long line at 1 m intervals taking samples typically from the depths of 0.05, 0.10, and 0.20 m. Altogether 9 profiles were measured.

In addition, visual observations on the cloud fraction and type were made once an hour usually from 08:00 to 22:00 UTC.

3.3 Large-scale measurements in 2003–2005

To study the variability of snow density, layering and temperature in the scale of climatically different regions in the study area, observations were made along the 310 km transect. The main transect was measured during two consecutive field seasons in austral summers 2003–2004 and 2004–2005. The observations yielded data from large-scale variability in snow density in both summers and large scale variability in snow temperature in the second summer. The large-scale variability of snow properties will be examined in the two climatically different regions: the ice shelf and the escarpment. In addition, a 50 km sub-section of the entire transect, covering the sub-glacial peninsula Näsen and part of the ice shelf (Fig. 1), was measured four times in two week intervals during 2004–2005. In summer 2003–2004, the variability of snow properties in the scale of 100 m (25 m pit interval) from the top 0.50 m was obtained

from measurements close to a weather station called AWS5, located 10 km south of Basen In an area of 100 m×75 m, eight pits were examined for density and layering.

3.4   Meteorological model products

We further utilized the operational analyses of the European Centre for Medium-Range
5 Weather Forecasts (ECMWF). The analyses are based on a global forecast model at T799 resolution (approximately 25 km in the horizontal). The temporal resolution is 6 h. Total precipitation (stratiform plus convective), 2-m air temperature, and 10-m wind speed were collected from the ECMWF data archive. The 2-m air temperature and 10-m wind speed are analyses based on 6-h forecasts (as the first-guess field) and
10 assimilated observations. No precipitation observations were, however, assimilated in the model. To avoid errors due to the model spin-up period (Tietäväinen and Vihma, 2008), we have made use of the 24-h precipitation forecasts.

4   Data analyses and results

4.1   Spatial and temporal variability close to Basen

15 On the basis of the measurements nearby Basen (Sect. 3.2), the mean temperature and density profiles were calculated for each snow pit and for each day. Then the mean profiles for the whole summers 2006–2007 and 2007–2008 were calculated. Standard deviations of temperature and density were calculated for each measurement depth to detect (a) intra-pit spatial variability, based on measurements made within a 15 min
20 time frame, (b) diurnal cycle, based on pit-averaged data, (c) day-to-day variability, based on diurnal means, and (d) total variability, including (a)–(c). Vertical profiles of these standard deviations were then analysed.

Further, the measurement conditions were classified to clear and cloudy according to the following rules: clear, if the total cloud fraction was 0–3/8, and cloudy, if the
25 total cloud fraction was 6–8/8. In the "clear" conditions, the clouds were usually high

or medium clouds, while in cloudy conditions the clouds were usually low or medium clouds. The profiles were further classified to morning profiles (measurements before 11:00 UTC) and evening profiles (18:00–22:00 UTC). Due to studies on the diurnal cycle of clear-sky albedo (not reported here), the snow measurements had highest priority on clear days, and in summer 2007–2008 no evening profiles happened to be measured during cloudy days.

Day-to-day temporal variability dominated the small-scale variability of snow temperature (standard deviation (std) exceeded 2 K in the uppermost centimetres), while the diurnal cycle was next important (std exceeds 1 K) and the intra-pit spatial variability was the smallest component (std less than 0.5 K at all depths) (Fig. 3). The total and day-to-day small-scale variability was largest at the snow surface, decreasing exponentially with an e-folding depth at 0.25 to 0.30 m. In summer 2006–2007, the diurnal cycle and intra-pit variability were, however, almost constant in the uppermost 0.07–0.08 m. In 2007–2008, less vertical profiles were measured, which may have affected the shape of the daily std. As new snow pits were made at locations typically 1–10 m from the previous ones, the results on day-to-day temporal variability and diurnal cycle also included some contribution from spatial variability. The temporal variability in the day-to-day scale was, however, much larger than the diurnal cycle, which demonstrates that the contribution from spatial variability (same for the day-to-day variability and diurnal cycle) must have been minor. This is supported by the results from the horizontal profile measurements (see below).

In 2007–2008 the snow temperatures were up to 1.4 K lower than in the previous summer (Fig. 3). This was due to lower air temperatures. At the depth of 0.90 m, the snow temperatures equalled. Taking into account the effect of density on heat conductivity (Sturm and Johnson, 1992; see below for the density differences), we can estimate that in summer 2006–2007 the downward heat flux in the uppermost 0.90 m of the snow pack was roughly twice as large as in the following summer. In that colder summer the day-to-day std in temperature was higher throughout the uppermost 0.90 m; at 0.025 m depth the difference was 0.6 K.

Spatial and temporal variability in Antarctic snow

T. Vihma et al.

The intra-pit variability in snow temperature in the spatial scale of 0.4 m was compared against data from the 10–20-m long horizontal profiles of snow temperatures with 1 m intervals. The latter data were analysed so that the std of snow temperature was calculated in the spatial scales of 2 m, 5 m, and for the length of the entire profile. The std increased with increasing horizontal scale. For the entire profile length, the std was 0.6, 0.5, and 0.4 K at the depths of 0.025, 0.10, and 0.20 m, respectively. These numbers are 50–190% larger than the intra-pit std shown in Fig. 3c.

The profile shape in the uppermost 0.30 m clearly depended on the cloud conditions (Fig. 4). Both during evenings and mornings, the mean cloudy-sky temperatures exceeded the mean clear-sky temperatures at all depths. Due to the strong surface radiative cooling during clear nights, the minimum temperatures at the depths of 0.05–0.3 m were observed in clear mornings (Fig. 4a). In the uppermost 0.10 m the morning mean clear-sky profile was warmer than at deeper layers because of the already increased penetration and absorption of shortwave radiation at the time of the measurements (before 11:00 UTC). The downward longwave radiation from clouds reduces the surface cooling during night and morning, thus in cloudy mornings the snow temperatures were up to 2.4 K higher than in clear mornings. The mean snow temperature difference under clear and cloudy skies was largest at the surface in the evening (about 3 K), because of the strong surface radiative cooling that was already occurring at the time of the measurements (between 18:00 and 22:00 UTC). The maximum temperature difference between morning and evening was observed at the depth of 0.10 m and was larger in clear skies than in cloudy skies (Fig. 4a), due to the larger diurnal variation of shortwave and longwave net radiation.

The day-to-day std (Fig. 4b) in the snow temperature increased towards the surface. The effects of the daytime and cloud cover were clear in the uppermost 0.20 m of the snow pack. At most measurement levels, the std were larger during clear-sky than cloudy conditions (difference up to 0.9 K) and larger during mornings than evenings (difference up to 0.5 K), except very close to the surface.

Title Page

Abstract | Introduction

Conclusions | References

Tables | Figures

◄◄ | ►►

◄ | ►

Back | Close

Full Screen / Esc

Printer-friendly Version

Interactive Discussion

The snow density profiles (Fig. 5) showed large differences between the two summers. In 2006–2007 the snow density was higher than in 2007–2008 in the whole 0.5 m layer, the maximum difference of 119 kg m^{-3} (40%) observed at the surface. In 2006–2007 the snow density had a minimum of 390 kg m^{-3} at the depth of 0.10 m

5 and the maximum of 445 kg m^{-3} at the depth of 0.50 m, while in 2007–2008 the density decreased monotonically from the depth of 0.40 m towards the surface value of 300 kg m^{-3}. Compared to these large differences, the std of snow density had, however, rather similar profiles (Fig. 5b and c). The std was largest in the uppermost 0.10 m. The day-to-day variability dominated, and the diurnal cycle was generally larger

10 than the intra-pit variability. The apparent diurnal cycle included, however, contribution from horizontal variability between the pits 1–10 m apart. The density measurements along the lines 10–20 m long suggested that it was probably responsible for most of the std (see below). Summer 2006–2007, when the snow density was higher, showed a larger apparent diurnal cycle and intra-pit variability than summer 2007–2008. The

15 total and day-to-day std in snow density decreased more at the depths of 0.10–0.20 m in 2007–2008, and again reached higher values at the depth of 0.50 m in 2007–2008.

According to the ECMWF operational analyses, the amount of snow fall in the Basen region in December–January 2007–2008 was 130% larger than during the same period in the previous summer. The large accumulation of new snow has probably been

20 the main reason for the lower density in summer 2007–2008. In addition, the colder weather with less metamorphosis in the snow pack may have contributed to the lower density. The large accumulation of new snow may also have contributed to the large day-to-day std in snow temperature in 2007–2008: new snow with low heat conductivity makes the near-surface snow temperatures more sensitive to synoptic-scale changes

25 in the air temperature.

The horizontal profile measurements along the lines 10–20 m long demonstrated that the std increased with horizontal scale (calculated for 2 m, 5 m, and the entire profile length), and at all scales reached its maximum at the depth of 0.10 m. For the entire profile length, the mean values at the depths of 0.025, 0.10, and 0.20 m were 36, 48,

and 24 kg m^{-3}, respectively. The numbers are 60–200% larger than the intra-pit std shown in Fig. 5c, demonstrating, as in the case of snow temperature, that results for the small-scale spatial variability are sensitive to the scale.

In the uppermost 0.10 m, the snow density showed dependency on the time of the day and cloud conditions (Fig. 6). The near-surface (0.01 m) density was highest in clear mornings and lowest in clear evenings. We interpret this so that during clear days the strongest melting and penetration of melt water reduced the near-surface density but increased the density at the depth of 0.10 m, seen in clear evenings in Fig. 6a. Further, the most efficient refreezing during clear nights increased the near-surface density, seen as largest values in clear mornings. The day-to-day std of snow density slightly increased towards the surface, at least in the uppermost 0.20 m (Fig. 6b). The high std in cloudy evenings was probably affected by the lack of data from 2007–2008.

In summer 2003–2004 eight 0.50 m deep snow profiles were measured at the AWS5 site 10 km south of Basen. The mean density increased with depth from 370 to 410 kg m^{-3} (Fig. 7a). The std varied a lot with depth in the range from 16 to 73 kg m^{-3} (Fig. 7c). The high variability in the std profiles compared to the ones acquired close to Basen is likely due to the small number of pits.

4.2 Spatial and inter-annual variability along the transect

Observations on the vertical profiles of the mean and std of snow temperature in summer 2004–2005 are presented in Fig. 8. The mean profiles clearly show the warmest snow in the ice shelf and coldest in Escarpment 2. Close to the surface, Escarpment 1 is 3.3 K and Escarpment 2 is 6.3 K colder than the ice shelf, but the differences decrease with depth. The mean altitudes are 63 m for the ice shelf, 469 m for Escarpment 1, and 1017 m Escarpment 2. Hence, with the dry-adiabatic lapse rate of 9.8 K/km, we calculate that the potential temperature is 0.7 K higher on Escarpment 1 than on the ice shelf, and 3.0 K higher on Escarpment 2 than on the ice shelf. See Sect. 5 for discussion on reasons for that. The horizontal std of snow temperatures is strongly controlled

by the std of altitude. The std of temperature at the depth of 0.025 m is 0.3, 3.1, and 1.3 °C for the ice shelf, Escarpment 1, and Escarpment 2, respectively, and the std of elevation in the three regions is 18, 271, and 101 m, respectively. The two std's at the depth of 0.025 m have a mutual correlation coefficient of 0.9995, and it exceeds 0.94

5 throughout the uppermost 0.50 m of snow.

Considering snow density, the 50 km subsection of the full 310 km transect was measured four times (17 and 23 December 2004, 2 and 14 January 2005). On each measurement day 6 to 8 pits were measured along the subsection. The mean density varied between 360 and 440 kg m^{-3} (Fig. 7b). The horizontal std of density was cal-

10 culated on the basis of time-averaged data from each pit. The std varied between 30 and 73 kg m^{-3} increasing with depth, although displaying rapid changes in the order of 10 to 30 kg m^{-3} (Fig. 7d). A precipitation event occurred on 7 to 8 January 2005. This probably generated noise in the std profile, as the depths of different layers changed and new surface micro-topography was created. The std for the spatial variability ac-

15 counts for 50–87% of the total variability in snow density along the 50 km subsection, calculated without time-averaging the data.

Over the 310 km transect the density ranged from 150 to 700 kg/m^3 with a mean density of 380 kg/m^3 and std of 70 kg/m^3. The mean and std profiles of the whole transect and the three areas (ice shelf, Escarpment 1 and Escarpment 2) are shown in

20 Fig. 7. In the 2003–2004 profiles, a low density layer was found near the surface between the depths of approximately 0.05 and 0.20 m. This pattern, which was stronger over the ice shelf but also visible in the other two areas, was not present in the mean density profiles obtained in 2004–2005, except slightly at Escarpment 1. We cannot account for all factors that have caused the differences in snow density profiles be-

25 tween the two years, but on the basis of the ECMWF operational analyses we can detect some weather patterns that may partly explain the differences. During summer 2004–2005 there was a precipitation event between 28 and 30 November, which was most pronounced over the ice shelf. In addition, the 2-m air temperature over the ice shelf was higher than during 2003–2004 campaign (Fig. 9), and therefore more melting

occurred. The penetration of melt water would decrease the density at the top of the snow cover and increase the density 0.10–0.30 m below the surface. These reasons probably contributed to the low mean density observed close to the surface of the ice shelf in 2004–2005 (Fig. 7b), and to the higher mean density at increasing depths.

5 Further, according to the ECMWF analysis, the uppermost 0.20 m of snow at the time of the field campaigns had accumulated mainly in autumn and winter in 2004, while mostly in late winter, spring, and early summer in 2003. The snow accumulated later in the season in 2003 was subjected to a shorter period of compression and erosion by the wind before the summer measurement campaign compared to the case in Decem-

10 ber 2004, and therefore it remained less dense in the layer between the depths of 0.05 and 0.20 m. The ECMWF-based wind speed itself did not show differences between the two years along the transect.

The higher air temperature in summer 2004–2005 and earlier snow accumulation in 2004 may also be at the origin of the larger spatial variability of density in 2004–

15 2005 compared to 2003–2004. The mean std profiles of density (Fig. 7c and d) show 5–15% larger values in 2004–2005 than in 2003–2004. The magnitude of variability of snow density in each separate section of the transect (corresponding to a spatial scale of 100 km) was generally between 40 to 80 kg/m^3 with the exception of the more homogeneous ice shelf during summer 2003–2004.

20 Another insight on the regional differences in the surface snow properties can be gained from the analysis of the subjective hardness observations. In Fig. 10 the layering observations are overlapped by density isolines. The hardness measurements repeated features similar to those in density. Over the ice shelf the snow layer was more horizontally homogeneous and had a better defined vertical structure than in the

25 escarpment region (compare also with Fig. 7c and d). The maps of the cumulative precipitation during the whole year before and during the measurement campaigns obtained from ECMWF operational analysis (Fig. 11) showed accumulation maxima over the ice-shelf and accumulation minimum in the Escarpment 2 region. The higher precipitation near the coast indeed reduced the vertical and horizontal heterogeneity,

which instead was more pronounced in layers that had been longer exposed to wind erosion and surface melting/sublimation.

The density is also affected by grain size and shape. Figure 12 shows the correlation between density and hardness in the top 0.50 m for both seasons 2003–2004 and 2004–2005. Calculated correlation coefficients for the two datasets were 0.55 and 0.43, with the significance level $p<0.01$. The co-variation of density and layering is also visible in Fig. 10 where the density isolines correspond well to the hardness features in the layering. Increase in density can usually be associated with increase in the degree of bonding of ice grains. Bonding of grains is also closely correlated with the penetration resistance of the snow, i.e. the hardness. The dependence between density and hardness is not straightforward, but depends on the metamorphism, which causes variation in their correlation (Dadic et al., 2008).

In 2003–2004, the section of the transect between sites 1142 and 1152 was the last to be measured, about one week after the other sections. The area had therefore developed a more complex layering, with some thick layers of ice due to re-freezing of penetrated melt water due to an intense melting period before the section measurements. The snow hardness displayed very different structure in the layering of this section compared to the neighbouring regions (Fig. 10, upper panel), with softening at the top 0.10 m due to surface melting and hardening at greater depths due to re-freezing.

Our measurements on spatial variability of snow density covered scales ranging from 0.4 m (intra-pit) to approximately 100 km (ice shelf and Escarpments 1 and 2). In Fig. 13 we summarize the results including for comparison the results of Sturm and Benson (2004) in the scale of 280 m. We see that the spatial std of snow density depends on the depth, but the dependence is not systematic.

5 Discussion

5.1 Spatial variability in snow density

The main message from Fig. 13 is the general increase of the std with increasing spatial scale. In this respect, the results of Sturm and Benson (2004) very well fit between
5   our results for smaller and larger scales (except at the depth of 0.02 m), although the values for the scale of 280 m were calculated on the basis of only three vertical profiles (Fig. 7 in Sturm and Benson, 2004) and the study region was different (Byrd station in West Antarctica). Sturm and Benson (2004) stressed the importance of wind in generating the maximum heterogeneity in the snow pack structure already at 100 m scale,
10 because it is the scale of many snow-drift features. Focusing on the vertically averaged values, we do not see any peak at the scale of 10^2 m. The conclusion of Sturm and Benson (2004) on the peak in heterogeneity in the scale of 10^2 m was, however, mostly based on results from the stratigraphic structure of the snow pack, instead of density data. We interpret the monotonous increase in the std resulting from the fact
15 that, when the scale increases, more processes generating heterogeneity start to be important and the processes acting already in smaller scales do not loose their importance. The most rapid increase in the spatial std of snow density takes place between the scales of 0.4 and 2 m, which is most probably related to the typical size of sastrugi (Goodwin, 1990): measurements with 0.4 m intervals are more often taken from the
20 same sastruga or from the same flat area between sastrugi than measurements with 2 m intervals.

Figure 13 shows that in spatial scales from 0.4 to 280 m, the highest standard deviations were observed close to the surface, but this does not hold over larger scales. The reason may lie in the erosion-deposition processes of different wind regimes. Watan-
25 abe (1978) reports detailed stratigraphical observations from the Mizuho plateau. Areas affected by strong katabatic winds create strong sastrugi formations during winter. Spring and summer time cyclonic precipitation events can level some of the rough surface creating less dens depositional layers and smoothing the surface, thus creating

Spatial and temporal variability in Antarctic snow

T. Vihma et al.

Title Page

Abstract | Introduction

Conclusions | References

Tables | Figures

◄ | ►

◄ | ►

Back | Close

Full Screen / Esc

Printer-friendly Version

Interactive Discussion

sub-surface density heterogeneity in the scale of ~1 m, the scale of strong sastrugi formations (Goodwin, 1990). This is also apparent in the stratigraphical observations from the region of our study. Both 2003–2004 and 2004–2005 observations show thick snow layers with low hardness over the ice shelf and more variability between the sites 1160 and 1175 (Fig. 10).

5.2 Effect of accumulation on snow density variability

The large-scale spatial variability of snow properties is strongly affected by the spatial variability in snow accumulation (Kärkäs et al., 2005). According to ECMWF forecasts, the spatial distribution and the amount of the one-year cumulative precipitation and the annual mean wind speed along the measured transect were very similar in the year preceding summers 2003–2004 and 2004–2005. However, in addition to precipitation also wind-driven snow deposition and erosion, wind- and solar radiation-induced sublimation, and melting affect the spatial variability in accumulation. The general spatial distribution in accumulation over the area maintains a rather typical pattern from year to year (Richardson et al., 1997; Reijmer and van den Broeke, 2003), but there are substantial variations in absolute accumulation between years (Richardson et al., 1997; Reijmer and van den Broeke, 2003; Richardson-Näslund, 2004). Generally, spatial variability in snow accumulation is lowest in the areas where the slope along the prevailing wind direction is low and accumulation is high (Frezzotti et al., 2007), thus, it is not surprising that we observed the lowest spatial variability in snow density over the ice shelf.

Frezzotti et al. (2007) and Eisen et al. (2008) discussed the spatial length scales of snow accumulation measurements in East Antarctica. They argue that in general the snow accumulation variability in scales 10^{-1} to 10^2 m is controlled by wind-induced surface features, i.e. sastrugi and dunes. Scales from 10^1 up to 10^4 m are governed by interaction of topography and wind and largest scales from 10^5 to 4×10^6 m are controlled by the synoptic climate. Our density data indicated a sharp increase in variability between the scales of 0.4 to 2 m, little increase up to 3×10^2 m scale, and a stronger

increase towards 10^5 m scale, except at the very surface (Fig. 13). The above suggests that the same factors control the horizontal variability in snow accumulation and density. On the basis of our results, observations in scale of 10^1 m can reasonably well represent the scale of 10^2 m, if there are no major topographic features. On the other hand, to better understand the spatial variability, more density observations are needed in spatial scales of 10^0–10^1 m and 10^3–10^4 m, and observations should also be made from depths larger than 0.50 m. If one is interested in the variability of climatically different areas, nested sampling with 10^0 to 10^1 m scales at each climate region would provide sufficient data to asses the influence of the climatic conditions.

Frezzotti et al. (2007) found that, on the annual scale, temporal variability in snow accumulation is inversely proportional to the amount of accumulation, decreasing to $\pm 10\%$ of the climatological mean accumulation only if accumulation is more than $750 \, \mathrm{kg \, m^{-2} \, y^{-1}}$. Considering that the accumulation rate over the ice shelf is lower than $400 \, \mathrm{mm \, w.e. \, y^{-1}}$ (Reijemer and van den Broeke, 2003), it is understandable that we observed large differences in snow density over the ice shelf between summers 2003–2004 and 2004–2005 (Fig. 7a and b). Indeed, the density of cyclones in the circumpolar trough has a local minimum in the region offshore our study area (Simmonds et al., 2003), thus precipitation events are less frequent than in other coastal areas. Hence, snow density and stratification are strongly affected by single precipitation events and inter-annual differences in air temperature and the timing of the precipitation events.

5.3 Spatial variability in snow temperature

Similarly to Granberg et al. (2009), who studied the same region, we observed that the potential temperatures of the upper snow pack decreased from inland (about 300 km from the coast) towards the coast. An analogous gradient in potential temperature perpendicular to the coast was also observed in a nearby area in Dronning Maud Land by van den Broeke et al. (1999). Granberg et al. (2009) suggested that the gradient is due to strong sublimation of wind-blown snow associated with katabatic winds, but did

not give any quantitative estimates of the sublimation. We note, however, that in the ECMWF operational analyses the potential temperature strongly decreases towards the ice shelf although the model does not include any parameterization of sublimation from blowing/drifting snow, but just the surface sublimation. Other arguments against the conclusion of Granberg et al. (2009) are that (a) the katabatic winds strongly atten-uate over the almost flat ice shelves (van den Broeke and van Lipzig, 2003; Renfrew, 2004) and (b) due to the vicinity of the sea and the larger cyclone activity, the air hu-midity over ice shelves is higher than over the interior (Tietäväinen and Vihma, 2008). These factors tend to reduce sublimation related to katabatic winds over ice shelves. As Hogan (1997), van den Broeke et al. (1999), and van den Broeke and van Lipzig (2003) we conclude that that the commonly observed decrease of potential temper-ature from escarpments towards ice shelves is caused by the accumulation of cold near-surface air brought by katabatic winds onto the ice shelves. In addition, when the katabatic winds attenuate over the ice shelves, the stratification increases resulting in further cooling of near-surface air. Further, the large-scale southward advection of warm air well above the atmospheric boundary layer, which balances the near-surface northward flow (King and Turner, 1997), has more potential to affect the snow tem-perature in higher escarpment regions than in low-lying ice shelves. Finally, model experiments of Lenaerts et al. (2010) suggested that even during large sublimation from drifting snow the effects on the snow surface temperature remain minor (Fig. 11 in Lenaerts et al., 2010). Analogously, we do not agree with Granberg et al. (2009) that higher potential temperatures at Högisen (Fig. 1) could be due to condensation heating in the katabatic layer as it ascends the hill.

5.4 Diurnal cycle

Although the day-to-day variability dominated the temporal variability in snow temper-ature and density, the results demonstrates that the diurnal cycle of snow temperature is clearly present in the study region during summer, when the sun did not set but its zenith angle varied from 50 to 89°. The penetration depth (0.20–0.25 m) of the diurnal

temperature cycle was close to that obtained by van Lipzig et al. (1999) at Svea in January 1993, by Jordan et al. (1989) for seasonal snow in New Hampshire, USA, in February, and by Cheng et al. (2008a,b) for snow on the Arctic sea ice in summer. In all these studies the diurnal range of solar zenith angle was between 36 and 43 degrees. High-resolution model experiments of Dadic et al. (2008) resulted in a penetration depth of 0.50 m for the Summit station in Greenland. It was supported by observations of a penetration depth down to 0.50 m on clear-sky days and down to 0.30 m on cloudy days. The diurnal range of solar zenith angle was no more than 36 degrees, but the penetration depth was probably increased by the stronger radiation at the high altitude of 3203 m a.s.l. Although melting occurred at the measurement site close to Basen during warmest days, it was so limited that it did not have detectable effects on the diurnal cycle. This was the case also during the Ice Station Polarstern in the western Weddell Sea in December 2004, but only for the diurnal cycle of the snow surface temperature (Vihma et al., 2009). Already at the depth of a few centimetres the snow was often wet with a very small or undetectable diurnal temperature cycle (Nicolaus et al., 2009).

5.5 Effects of clouds

During clear evenings, the subsurface temperature maxima observed at the measurement site close to Basen was located at the depth of 0.10 m (Fig. 4a). Penetration of solar radiation in the snow pack tends to generate the subsurface maxima closer to the surface, typically at the depths of 0.02–0.06 m, depending on the extinction coefficient (Cheng et al., 2003, 2008a). The lower depth observed must be a result of the measurement time in the evening, when the surface cooling due to the loss of longwave radiation had already propagated to the upper measurement levels via heat conduction. The shape of the clear-evening temperature profile is convex (Fig. 4a), resembling the clear-evening profile of Jordan et al. (1989). This suggests that the shape of the profile is controlled by heat conduction instead of heat advection in the air pores in the snow pack. This is typical for wind-packed snow and polar firn (Albert and McGilvary,

Spatial and temporal variability in Antarctic snow

T. Vihma et al.

1992; Brandt and Warren, 1997). Opposite cases of advection-dominated high porosity snow are typically associated with concave profiles (Jordan et al., 2008).

Clouds strongly modulate the amount of shortwave radiation reaching the surface and penetrating into the snowpack, therefore it is not surprising that they had a sig-

5 nificant effect on the temperature profiles of the uppermost few decimetres of snow. Bakermans and Jamieson (2009) found that the incoming shortwave radiation, parameterized as a function of cloud cover fraction, was the only significant parameter, among those tested, which could be used as a predictor when parameterizing the daytime subsurface warming at the depth of 0.10–0.15 m in a Canadian glacier. In the

10 uppermost 0.10 m, the subsurface temperatures were 2–3 °C higher in overcast days than in clear-sky days. With a high surface albedo (>0.8) and solar zenith angles, the increase of net longwave irradiance at the surface due to clouds dominates over the decrease of net shortwave irradiance (Shupe and Intrieri, 2004; van den Broeke et al., 2006), which results in a cloud radiative warming of the surface. Indeed, the average

15 subsurface heat flux calculated by van den Broeke et al. (2006) for our study area during three consecutive summers (1998–2001) was about $0\,\mathrm{W\,m^{-2}}$ and $5\,\mathrm{W\,m^{-2}}$ (positive downward) in clear and overcast skies, respectively.

The reason for the observed larger day-to-day variability of the clear-sky temperature profiles compared to the cloudy profiles (Fig. 4b) can be explained as follows. While

20 temperature maxima were close to the melting point in most of clear and cloudy days, temperature minima were much lower in clear days, due to the stronger nocturnal heat loss. Thus, the daily excursion of surface temperature was 8–12 °C larger in clear than cloudy days, and day-to-day differences in the exact timing of the temperature measurements between 18:00 and 22:00 UTC generated the larger std in clear compared

25 to cloudy days.

Title Page

Abstract | Introduction

Conclusions | References

Tables | Figures

◄◄ | ►►

◄ | ►

Back | Close

Full Screen / Esc

Printer-friendly Version

Interactive Discussion

5.6 Comparison of spatial and temporal variability

Considering the relative importance of spatial and temporal variations, in the 50–100 km scale the horizontal variability of snow density increased with depth, whereas in the smaller scales it decreased with depth. In the intra-pit scale of 0.4 m, however, the relative magnitude of horizontal compared to day-to-day variability increased with depth. This was due to the decrease of temporal variability with depth. In the intra-pit scale, the temporal variability (dominated by the day-to-day variability) exceeded the horizontal variability throughout the uppermost 0.50 m layer. Assuming that the temporal variability of the snow density shown in Fig. 5b and c is representative also for the environment of the large-scale transect measurements, it exceeded the large-scale horizontal variability (Fig. 7d) only in the uppermost centimetres, but the horizontal variability dominated already at the depth of 0.10 m.

Considering the std of snow temperature (Fig. 3b and c), the temporal variability, both in day-to-day scale and diurnal cycle, exceeded the horizontal variability in the intra-pit scale of 0.4 m throughout the 0.50 m layer. In the uppermost 0.40 m, this was also the case comparing the total and day-to-day temporal variability against the horizontal variability along the ice shelf and Escarpment 2 (Figs. 3 and 8, assuming that the Basen measurements represent the temporal variability also along the transect). In Escarpment 1, however, the large-scale horizontal variability dominated. Both in the small and large scale, the relative magnitude of horizontal variability was largest in the lower part of the 0.50 m layer. This was due to temporal variability increasing more strongly towards the surface. Accordingly, the main difference between the variability of snow density and temperature was that the relative importance of horizontal variability was larger for density. This we interpreted as a result of (a) the role of heat conduction that more effectively smoothes horizontal variations in temperature than in density and (b) variability in the radiative and turbulent surface fluxes that more directly generates temporal variations in temperature than in density.

Title Page

Abstract | Introduction

Conclusions | References

Tables | Figures

|◄ | ►|

◄ | ►

Back | Close

Full Screen / Esc

Printer-friendly Version

Interactive Discussion

6 Conclusions

We observed large inter-annual variations in the snow pack. In 2007–2008 the snow temperatures were up to 1.4 K lower than in the previous summer. In 2006–2007 the snow density was higher than in 2007–2008 in the whole 0.5 m layer, the maximum difference of 40% observed at the surface. These differences were due to inter-annual differences in air temperature and the timing of the precipitation events. The snow layering detected by subjective hardness observations was well in agreement with density observations.

Despite of summer, the cloud radiative forcing was positive in the study region. Temperature maxima were close to the melting point in most of clear and cloudy days, but temperature minima were much lower in clear days. The effects of cloud cover on snow temperature (density) were clearly detected in the uppermost 0.30 m (0.10 m). Although melting occurred at the measurement site close to Basen during warmest days, it did not have detectable effects on the diurnal temperature cycle, which penetrated to the depth of 0.20–0.25 m.

Both in the intra-pit and transect scales, the ratio of horizontal to temporal variability increased with depth, as the temporal variability decreased more strongly with depth. In the intra-pit scale the temporal variability in snow density exceeded the horizontal variability throughout the uppermost 0.50 m layer, but in the 100-km scale only in the uppermost centimetres. For the snow temperature close to Basen, day-to-day variability dominated (std>2 K in the uppermost centimetres), while the diurnal cycle was next important (std>1 K) and horizontal variability in the scale of 0.4 to 10 m was smallest (std≤0.6 K). Day-to-day temporal variability exceeded the horizontal variability also along the ice shelf and Escarpment 2. In Escarpment 1, however, the large-scale horizontal variability dominated. The main difference between the variability of snow density and temperature was that the relative importance of horizontal variability was larger for density, probably mostly due to the effects of radiative and turbulent surface fluxes in more directly generating temporal variations in temperature than in density.

The horizontal std of snow density and temperature increased with the spatial scale. The most rapid increase took place between the scales of 0.4 and 2 m, which is most probably related to the typical size of sastrugi. In 10^5 m scale, the std of snow temperatures was strongly controlled by the std of surface altitude. Considering future field work, our results suggest that observations in the scale of 10^1 m can reasonably well represent the scale of 10^2 m, if there are no major topographic features. On the other hand, to better understand the spatial variability, more density observations are needed in spatial scales of 10^0–10^1 m and 10^3–10^4 m, and observations should also be made from depths larger than 0.50 m. Further, in low-accumulation sites, relatively small differences in accumulation rates ($<$40 mm w.e. y^{-1}) cause differences in the residence time of the snow crystals in the near-surface layer, which may result in large differences in snow physical properties, as grain size and thermal conductivity, without significant differences in density (Courville et al., 2007). Therefore, in future field experiments addressing the surface energy balance, we should consider to include the thermal conductivity of snow among the snow pit measurements.

References

Albert, M. R. and McGilvary, W. R.: Thermal effects due to air flow and vapour transport in dry snow, J. Glaciol., 38, 273–281, 1992.

Bakermans, L. and Jamieson, B.: Swarm: a simple regression model to estimate near-surface snowpack warming for back-country avalanche forecasting, Cold Reg. Sci. Technol., 59, 133–142, 2009.

Brandt, R. E. and Warren, S. G.: Temperature measurements and heat transfer in near-surface snow at the South Pole, J. Glaciol., 43, 339–351, 1997.

Cheng, B., Launiainen, J., and Vihma, T.: Modelling of superimposed ice formation and sub-surface melting in the Baltic Sea, Geophysica, 39, 31–50, 2003.

Cheng, B., Zhang, Z., Vihma, T., Johansson, M., Bian, L., Li, Z., and Wu, H.: Model experiments on snow and ice thermodynamics in the Arctic Ocean with CHINARE2003 data, J. Geophys. Res., 113, C09020, doi:10.1029/2007JC004654, 2008a.

Cheng, B., Vihma, T., Zhang, Z., Li, Z., and Wu, H.: Snow and sea ice thermodynamics in the Arctic: model validation and sensitivity study against SHEBA data, Chinese Journal of Polar Science, 19, 108–122, 2008b.

Colbeck, S.: Layered character of snow covers, Rev. Geophys., 29, 81–96, 1991.

Colbeck, S. C., Akitaya, E., Armstrong, R., Gubler, H., Lafeuille, J., Lied, K., McClung, D., and Morris, E.: International classification for seasonal snow on the ground, International Commision on Snow and Ice of the International Association of Scientific Hydrology, World Data Centre – Association for Glaciology, Univeristy of Colorado, Boulder, CO, 23 pp., 1990.

Courville, Z. R., Albert, M. R., Fahnestock, M. A., Cathles IV, L. M., and Shuman, C. A.: Impacts of an accumulation hiatus on the physical properties of firn at a low-accumulation polar site, J. Geophys. Res., 112, F02030, doi:10.1029/2005JF000429, 2007.

Dadic, R., Schneebeli, M., Lehning, M., Hutterli, M. A., and Ohmura, A.: Impact of the mi-crostructure of snow on its temperature: a model validation with measurements from Sum-mit, Greenland, J. Geophys. Res., 113, D14303, doi:10.1029/2007JD009562, 2008.

Eisen, O., Frezzotti, M., Genthon, C., et al.: Ground-based measurements of spatial and temporal variability of snow accumulation in East Antarctica, Rev. Geophys., 46, RG2001, doi:10.1029/2006RG000218, 2008.

Frezzotti, M., Gandolfi, S., La Marca, F., and Urbini, S.: Snow dunes and glazed surfaces in Antarctica: new field and remote-sensing data, Ann. Glaciol., 34, 81–88, 2002a.

Frezzotti, M., Gandolfi, S., and Urbini, S.: Snow megadunes in Antarcitca: sedimentary struc-ture and genesis, J. Geophys Res., 107, 4344, doi:10.1029/2001JD000673, 2002b.

Frezzotti, M., Pourchet, M., Flora, O., Gandolfi, S., Gay, M., Urbini, S., Vincent, C., Becagli, S., Gragnani, R., Proposito, M., Severi, M., Traversi, R., Udisti, R., and Fily, M.: New estimations of precipitation and surface sublimation in East Antarctica from snow accumulation measure-ments, Clim. Dynam., 23, 803–813, doi:10.1007/s00382-004-0462-5, 2004.

Frezzotti, M., Urbini, S., Proposito, M., Scarchilli, C., and Gandolfi, S.: Spatial and temporal variability of surface mass balance near Talos Dome, East Antarctica, J. Geophys. Res., 112, F02032, doi:10.1029/2006JF000638, 2007.

Spatial and temporal variability in Antarctic snow

T. Vihma et al.

Title Page

Abstract	Introduction
Conclusions	References
Tables	Figures

◄ ►

◄ ►

Back | Close

Full Screen / Esc

Printer-friendly Version

Interactive Discussion

Frey, M. M., Hutterli, M. A., Chen, G., Sjostedt, S. J., Burkhart, J. F., Friel, D. K., and Bales, R. C.: Contrasting atmospheric boundary layer chemistry of methylhydroperoxide (CH_3OOH) and hydrogen peroxide (H_2O_2) above polar snow, Atmos. Chem. Phys., 9, 3261–3276, doi:10.5194/acp-9-3261-2009, 2009.

5 Goodwin, I. D.: Snow accumulation and surface topography in the katabatic zone of Eastern Wilkes Land, Antarctica, Antarct. Sci., 2, 235–242, 1990.

Granberg, H., Cliche, P., Mattila, O.-P., Kanto, E., and Leppäranta, M.: A snow sensor experiment in Dronning Maud Land, Antarctica, J. Glaciol., 55, 1041–1051, 2009.

Granskog, M., Vihma, T., Pirazzini, R., and Cheng, B.: Superimposed ice formation and surface
10 fluxes on sea ice during the spring melt-freeze period in the Baltic Sea, J. Glaciol., 52, 119–127, 2006.

Harper, J. T. and Bradford, J. H.: Snow stratigraphy over a uniform depositional surface: spatial variability and measurement tools, Cold Reg. Sci. Technol., 37, 289–298, 2003.

Hogan, A.: A synthesis of warm air advection to the South Polar Plateau, J. Geophys. Res.,
15 102, 14009–14020, 1997.

Jordan, R. E., O'Brian, H., and Albert, M. R.: Snow as a thermal background: preliminary results from the 1987 field test, in: Proc., Snow Symposium VII. US Army Cold Regions Research and Engineering Laboratory, Hanover, NH, Special Report 89-7, 5–24, 1989.

Jordan, R. E., Albert, M. R., and Brun, E.: Physical processes within the snow cover and their
20 parameterization, in: Snow and Climate. Physical Processes, Surface Energy Exchange and Modeling, edited by: Armstrong, R. E. and Brun, E., Cambridge University Press, 222 pp., 2008.

Kärkäs, E.: Meteorological conditions of the Basen nunatak in western Dronning Maud Land, Antarctica, during the years 1989–2001, Geophysica, 40, 39–52, 2004.

25 Kärkäs, E., Granberg, H., Kanto, K., Rasmus, K., Lavoie, C., and Leppäranta, M.: Physical properties of the seasonal snow cover in Dronning Maud Land, East Antarctica, Ann. Glaciol., 34, 89–94, 2002.

Kärkäs, E., Martma, T., and Sonninen, E.: Physical properties and stratigraphy of surface snow in western Dronning Maud Land, Antarctica, Polar Res., 24, 55–67, 2005.

30 King., J. C. and Turner, J.: Antarctic Meteorology and Climatology, University Press Cambridge, Cambridge, 409 pp., 1997.

Kronholm, K., Schneebeli, M., and Schweizer, J.: Spatial variability of micropenetration resistance in snow layers on a small slope, Ann. Glaciol., 38, 202–208, 2004.

Spatial and temporal variability in Antarctic snow

T. Vihma et al.

Title Page

Abstract	Introduction
Conclusions	References
Tables	Figures

| ◄◄ | ►► |
| ◄ | ► |

| Back | Close |

Full Screen / Esc

Printer-friendly Version

Interactive Discussion

Launiainen, J., Uotila, J., Vihma, T., Taalas, P., Karlsson, K., and Siivola, J.: Meteorological observations at the Aboa base 1989–1994, Antarctic Reports of Finland, No 5, Ministry of Trade and Industry, Helsinki, 27 pp., 1995.

Lenaerts, J. T. M., van den Broeke, M. R., Déry, S. J., König-Langlo, G., Ettema, J., and Munneke, P. K.: Modelling snowdrift sublimation on an Antarctic ice shelf, The Cryosphere, 4, 179–190, doi:10.5194/tc-4-179-2010, 2010.

Mäkynen, M., Cheng, B., Similä, M., Vihma, T., and Hallikainen, M.: Comparisons between SAR backscattering coefficient and results of a thermodynamic snow/ice model for the Baltic Sea land-fast sea ice, IEEE T. Geosci. Remote, 45, 1131–1141, 2007.

Meløysund, V., Leira, B., Høiseth, K. V., and Lisø, K. R.: Predicting snow density using meteorological data, Meteorol. Appl., 14, 413–423, doi:10.1002/met.40, 2007.

Nicolaus, M., Haas, C., and Willmes, S.: Evolution of first-year and second-year snow properties on sea ice in the Weddell Sea during spring-summer transition, J. Geophys. Res., 114, D17109, doi:10.1029/2008JD011227, 2009.

Pirazzini, R.: Surface albedo measurements over Antarctic sites in summer, J. Geophys. Res., 109, D20118, doi:10.1029/2004JD004617, 2004.

Reijmer, C. H. and Oerlemans, J.: Temporal and spatial variability of the surface energy balance in Dronning Maud Land, East Antarctica, J. Geophys. Res., 107, 4759, doi:10.1029/2000JD000110, 2002.

Reijmer C. H., van den Broeke, M. R., and Scheele, M. P.: Air parcel trajectories and snowfall related in five deep drilling locations in Antarctica based on the ERA-15 dataset, J. Climate, 15, 1957–1968, 2002.

Reijmer, C. H. and van den Broeke, M. R.: Temporal and spatial variability of the surface mass balance in Dronning Maud Land, Antarctica, as derived from automatic weather stations, J. Glaciol., 49, 512–520, 2003.

Renfrew, I. A.: The dynamics of idealized katabatic flow over a moderate slope and ice shelf, Q. J. Roy. Meteor. Soc., 130, 1023–1045, 2004.

Richardson, C., Aarholt, E., Hamran, S. E., Holmlund, P., and Isaksson, E.: Spatial distribution of snow in western Dronning Maud Land, East Antarctica, mapped by a ground-based snow radar, J. Geophys. Res., 102, 20343–20353, 1997.

Richardson-Näslund, C.: Spatial characteristics of snow accumulation in Dronning Maud Land, Antarctica, Global Planet. Change, 42, 31–43, 2004.

Spatial and temporal variability in Antarctic snow

T. Vihma et al.

Title Page

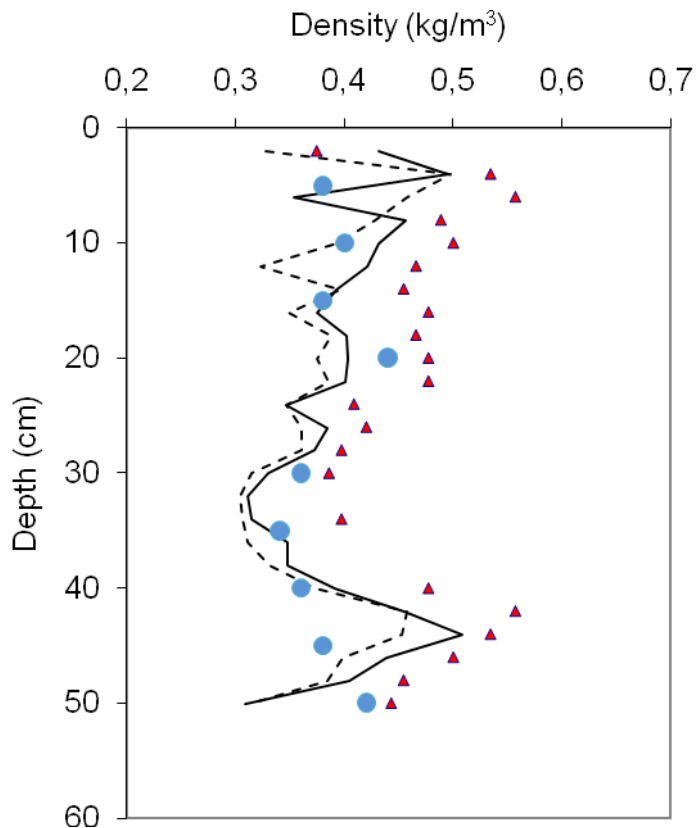| Abstract | Introduction |
| Conclusions | References |
| Tables | Figures |

|◄ | ►|

◄ | ►

Back | Close

Full Screen / Esc

Printer-friendly Version

Interactive Discussion

Shupe, M. D. and Intrieri, J. M.: Cloud radiative forcing of the Arctic surface: the influence of cloud properties, surface albedo, and solar zenith angle, J. Climate, 17, 616–628, 2004.

Sihvola, A. and Tiuri, M.: Snow fork for field determination of density and wetness profiles of a snow pack, IEEE T. Geosci. Remote., GE-24, 717–721, 1986.

5 Simmonds, I., Keay, K., and Lim, E.-P.: Synoptic activity in the seas around Antarctica, Mon. Weather Rev., 131, 272–288, 2003.

Sturm, M. and Benson, C.: Scales of spatial heterogeneity for perennial and seasonal snow layers, Ann. Glaciol., 38, 253–260, 2004.

Sturm, M. and Johnson, J. B.: Thermal conductivity measurements on depth hoar, J. Geophys.
10 Res., 97, 2129–2139, 1992.

Tietäväinen, H. and Vihma, T.: Atmospheric moisture budget over Antarctica and Southern Ocean on the basis of ERA-40 reanalysis, Int. J. Climatol., 28, 1977–1995, doi:10.1002/joc.1684, 2008.

Van den Broeke, M., Reijmer, C., van As, D., and Boot, W.: Daily cycle of the surface energy
15 balance in Antarctica and the influence of clouds, Int. J. Climatol., 26, 1587–1605, 2006.

Van den Broeke, M., Reijmer, C., and van de Wal, R.: Surface radiation balance in Antarctica as measured with automatic weather stations, J. Geophys. Res., 109, D09103, doi:10.1029/2003JD004394, 2004.

Van den Broeke, M. and van Lipzig, N. P. M.: Factors controlling the near-surface wind field in
20 Antarctica, Mon. Weather Rev., 131, 733–743, 2003.

Van de Broeke, M. R., Winther, J.-G., Isaksson, E., Pinglot, J. F., Karlöf, L., Eiken, T., and Conrads, L.: Climate variables along a traverse line in Dronning Maud Land, East Antarctica, J. Glaciol., 45, 295–302, 1999.

Van Lipzig, N. P. M., van Meijgaard, E., and Oerlemans, J.: Evaluation of a regional atmospheric
25 model using measurements of surface heat exchange processes from a site in Antarctica, Mon. Weather Rev., 127, 1994–2011, 1999.

Vihma, T., Johansson, M. M., and Launiainen, J.: Radiative and turbulent surface heat fluxes over sea ice in the western Weddell Sea in early summer, J. Geophys. Res., 114, C04019, doi:10.1029/2008JC004995, 2009.

30 Watanabe, O.: Stratigraphic studies of the snow cover in Mizuho Plateau, Memoirs of National Institute of Polar Research, 7, 44–62, 1978.

Title Page

Abstract | Introduction

Conclusions | References

Tables | Figures

◄ | ►

◄ | ►

Back | Close

Full Screen / Esc

Printer-friendly Version

Interactive Discussion

T. Vihma et al.

Table 1. Nomination of classes of subjective hardness, adopted from Colbeck et al. (1990).

Class name	Hand test	Hardness
1	Fist	Very low
2	4 fingers	Low
3	1 finger	Medium
4	Pencil	High
5	Knife	Very high
6	–	Ice
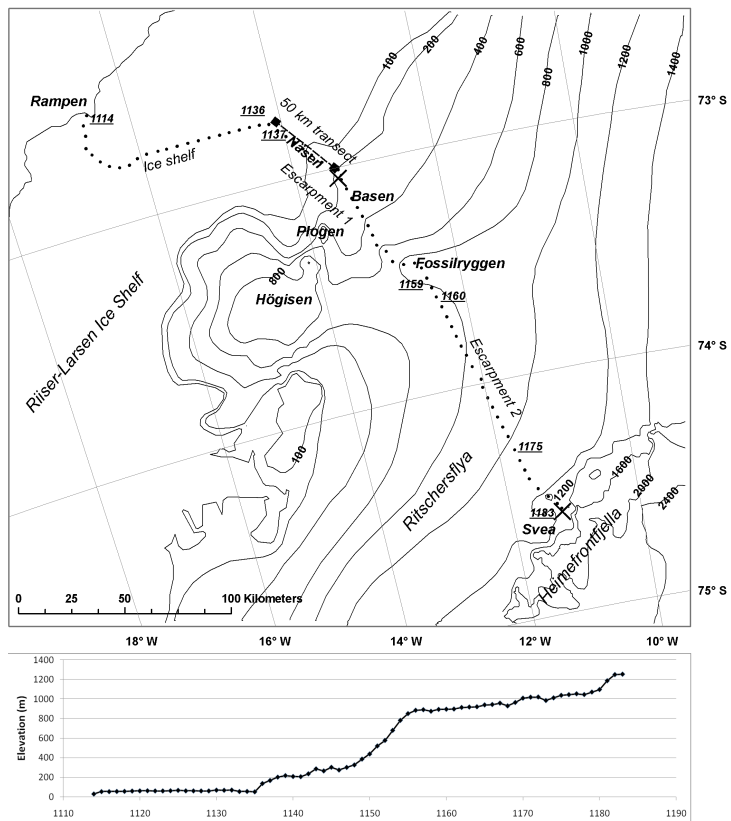
Fig. 1. Map of the research area and profile of elevation for the long transect. Each measurement site along thetransect is identified by the code 11 followed by a progressive number, from 1 at the coast to 83 at the innermost site (sites 1114, 1136, 1137, 1159, 1160, and 1183 are marked in the map). The region marked as Ice shelf extends from 1114 to 1136, the Escarpment 1 from 1137 to 1159, and Escarpment 2 from 1160 to 1183. The crosses mark the locations of Basen and Svea Stations.

Fig. 2. Validation of the snow density measurements using the snow fork. The two lines describe measurements of two different sensor heads of the snow fork. The circles give the values of traditional snow cylinder and triangles display measurements of melted samples from fine scale measurements.
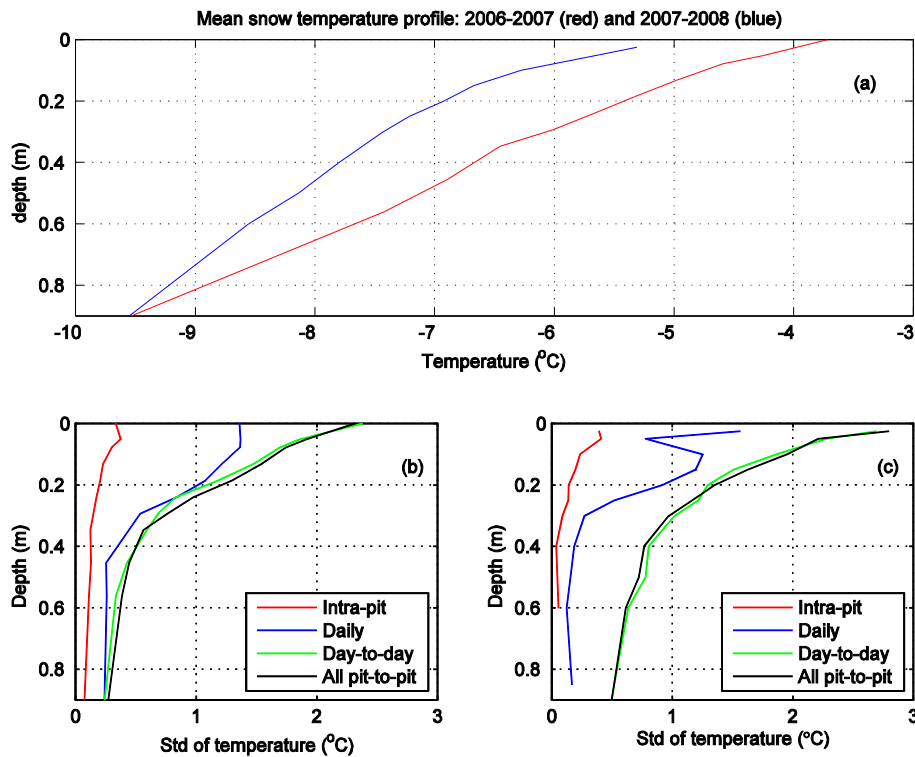
Fig. 3. Vertical profiles of **(a)** mean snow temperatures in summers 2006–2007 and 2007–2008, **(b)** standard deviations of snow temperature at different scales in summer 2006–2007, and **(c)** summer 2007–2008.
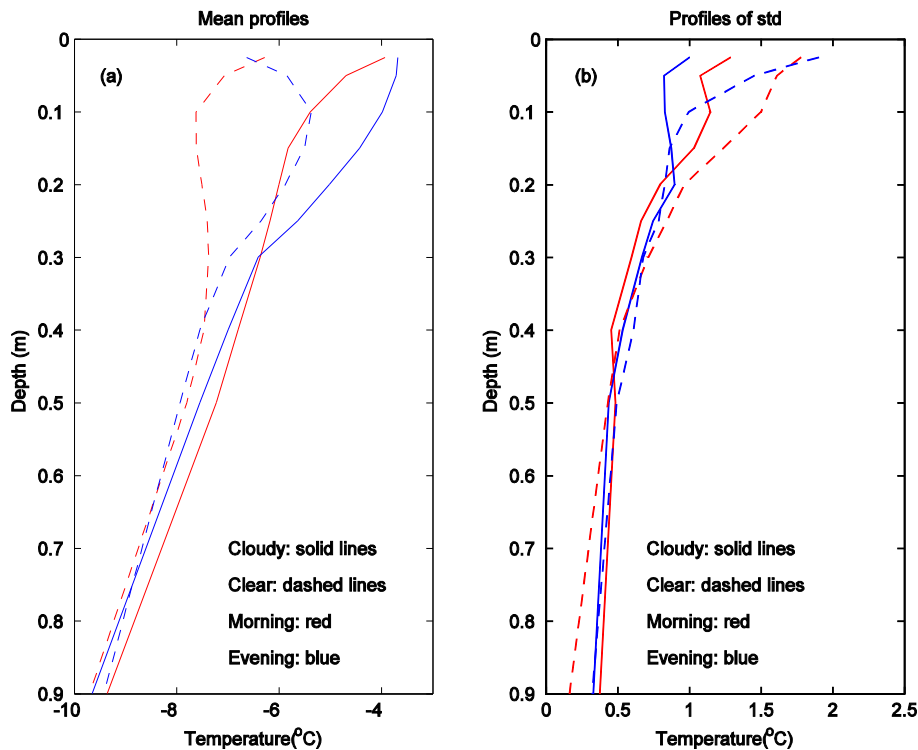
Fig. 4. Mean profiles of **(a)** snow temperature and **(b)** day-to-day standard deviation of snow temperature, averaged over the two summers but calculated separately for cloudy mornings, clear mornings, cloudy evenings, and clear evenings.

Title Page

Abstract | Introduction

Conclusions | References

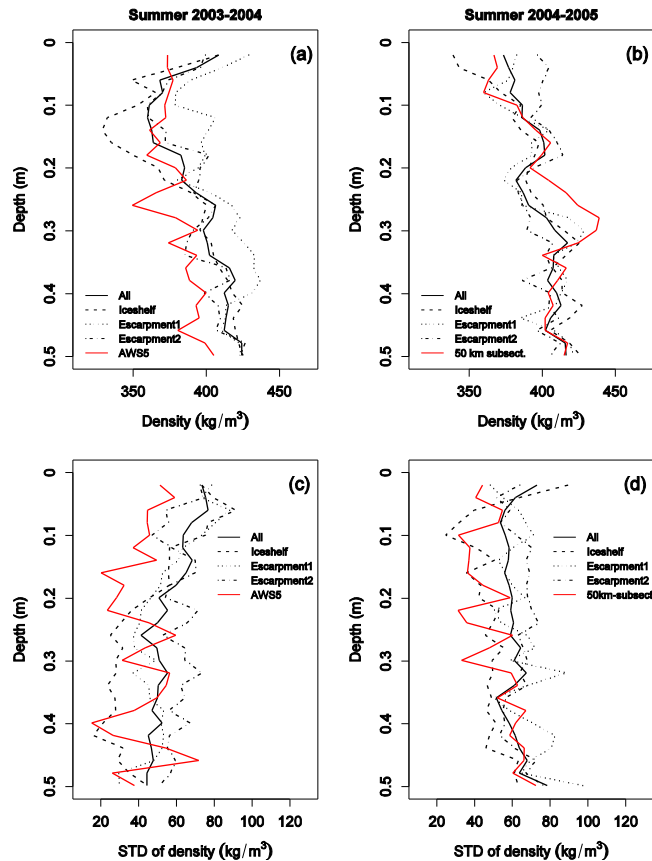Tables | Figures

◄◄ | ►►

◄ | ►

Back | Close

Full Screen / Esc

Printer-friendly Version

Interactive Discussion
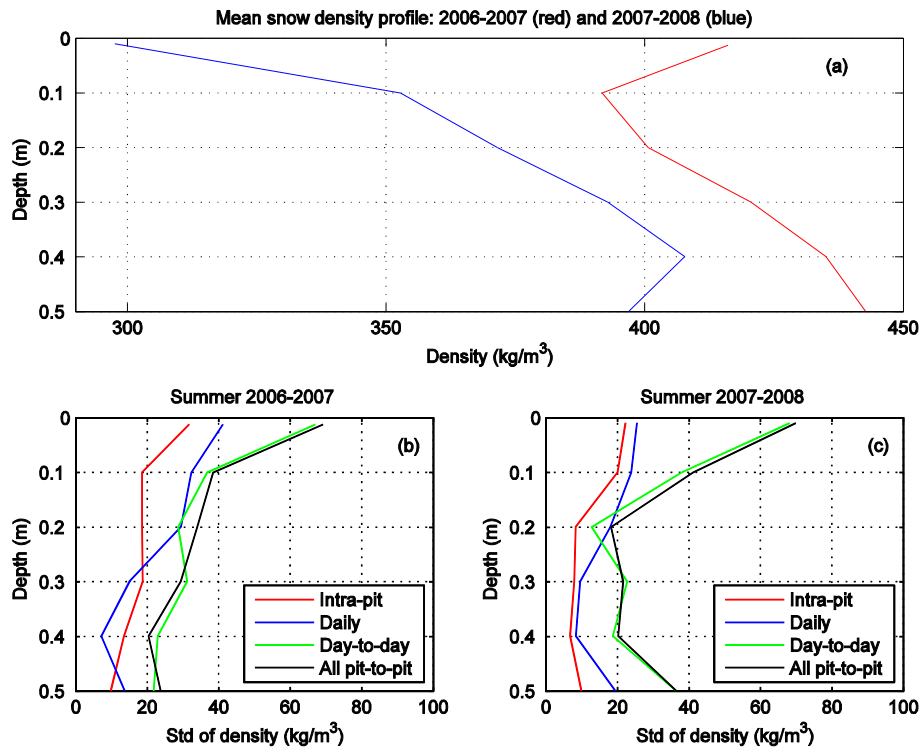
Fig. 5. Vertical profiles of **(a)** mean snow density in summers 2006–2007 and 2007–2008, **(b)** standard deviations of snow density at different scales in summer 2006–2007, and **(c)** summer 2007–2008.
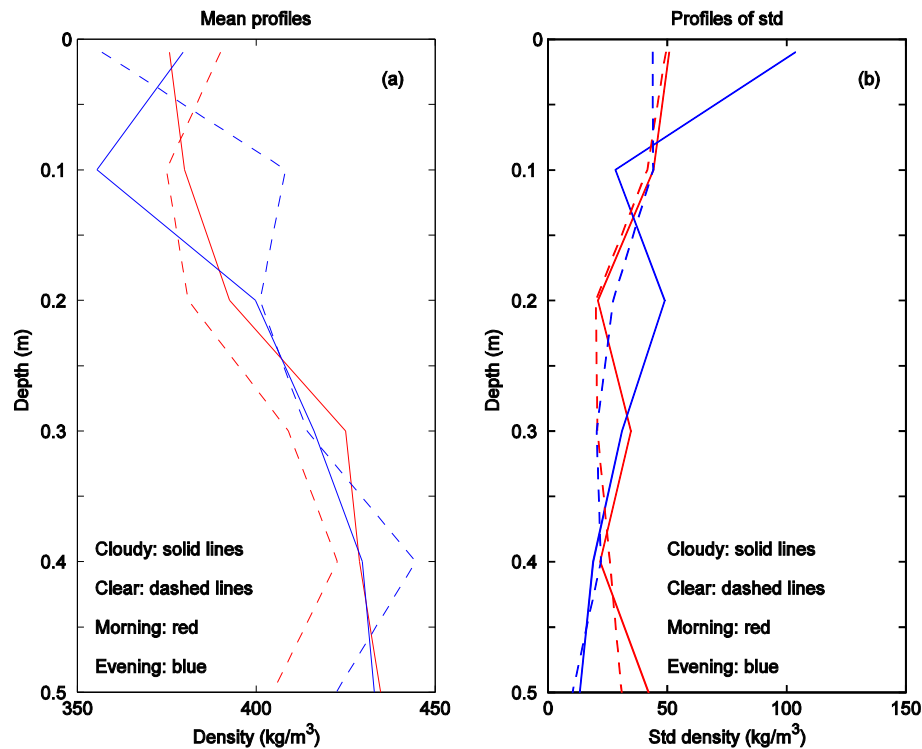
Fig. 6. Mean profiles of **(a)** snow density and **(b)** day-to-day standard deviation of snow density, averaged over the two summers but calculated separately for cloudy mornings, clear mornings, cloudy evenings, and clear evenings.

Fig. 7. Profiles of mean density (upper panels) and standard deviation of density (lower panels) from the 310 km transect (from the entire transect and from separate sections of the transect), from the site of the AWS5 and from the 50 km subsection during seasons 2003/04 (left) and 2004/05 (right).

Title Page

Abstract | Introduction

Conclusions | References

Tables | Figures

◄ | ►

◄ | ►

Back | Close

Full Screen / Esc

Printer-friendly Version

Interactive Discussion
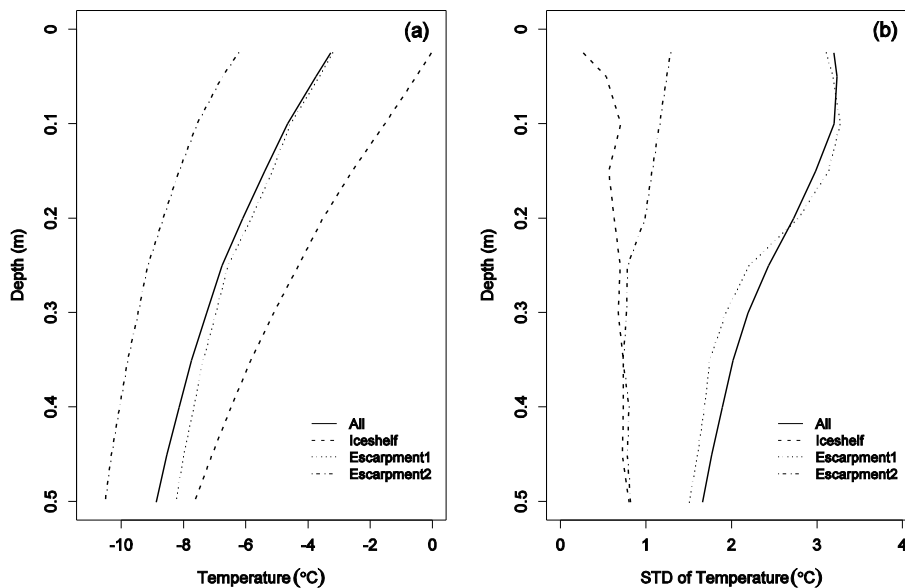
Fig. 8. Profiles of mean temperature (left) and horizontal standard deviation of temperature (right) from the 310 km transect (from the entire transect and from separate sections of the transect) during the season 2004/05.

Title Page

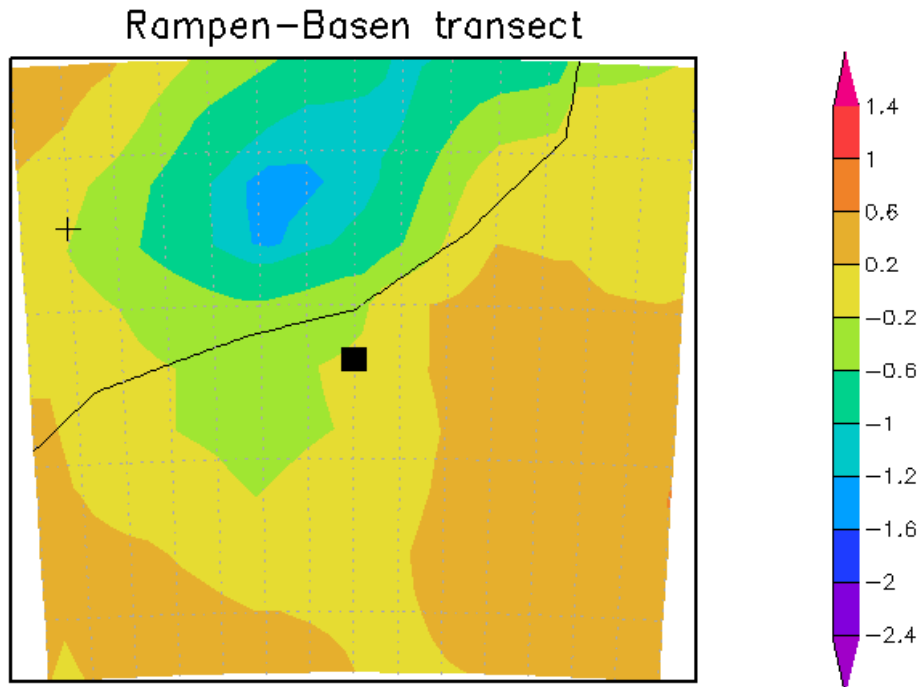Abstract | Introduction

Conclusions | References

Tables | Figures

|◄ | ►|

◄ | ►

Back | Close

Full Screen / Esc

Printer-friendly Version

Interactive Discussion

Fig. 9. Difference in 2-m air temperature between the two measurement campaigns (2003/04–2004/05) during the Rampen-Basen transect. Basen is marked by the square and Rampen by the cross.

Title Page

Abstract | Introduction

Conclusions | References

Tables | Figures

|◄ | ►|

◄ | ►

Back | Close

Full Screen / Esc

Printer-friendly Version

Interactive Discussion
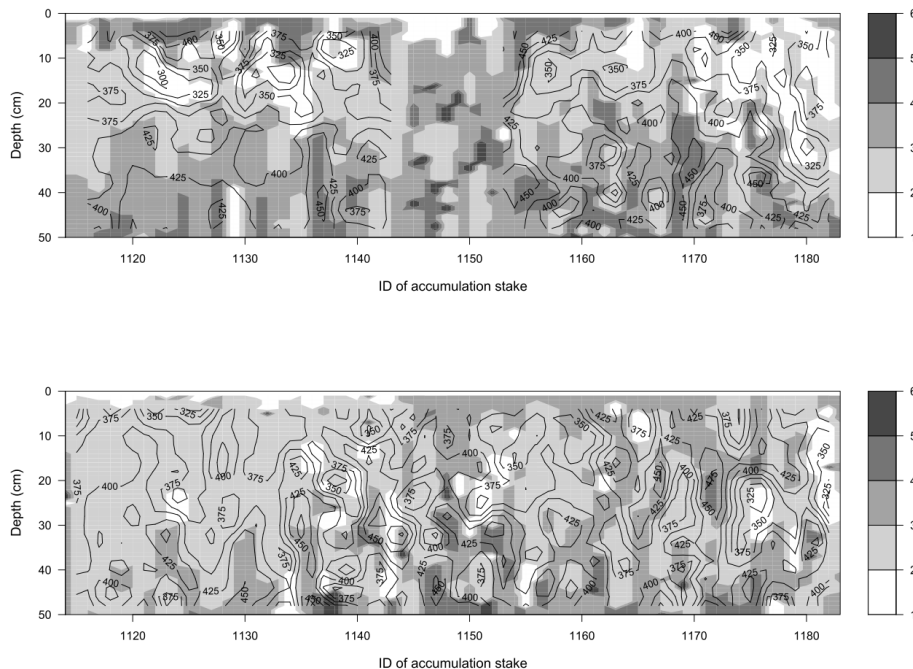
Fig. 10. Subjective layer hardness (grey scale, see Table 1) from the shallow snow pit transect from 2003/04 (top) and 2004/05 (bottom). On the x-axis are the ordinal numbers corresponding to the snow pit sites, located 5 km apart from each other (see Fig. 1). The contour lines mark the snow density (in $kg\,m^{-3}$).

Spatial and temporal variability in Antarctic snow

T. Vihma et al.

Title Page

Abstract	Introduction
Conclusions	References
Tables	Figures

|◄ | ►|

◄ | ►

Back | Close

Full Screen / Esc

Printer-friendly Version

Interactive Discussion

Title Page

Abstract | Introduction

Conclusions | References

Tables | Figures

|◄ | ►|

◄ | ►

Back | Close

Full Screen / Esc

Printer-friendly Version

Interactive Discussion
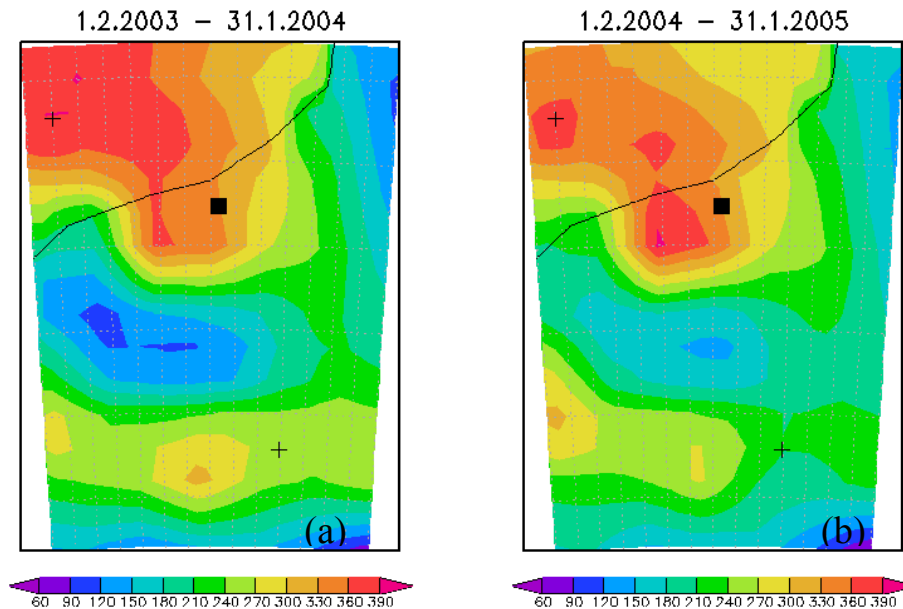
Fig. 11. Cumulative precipitation in the measurement area (72–75° S, 343–350° E) according to ECMWF operational 24-h forecasts for **(a)** an annual period ending on 31 January 2004 (end of the measurement campaign) and **(b)** an annual period ending on 31 January 2005 (end of the measurement campaign). The upper cross, the square, and the lower cross mark the location of Rampen, Aboa, and Svea, respectively.
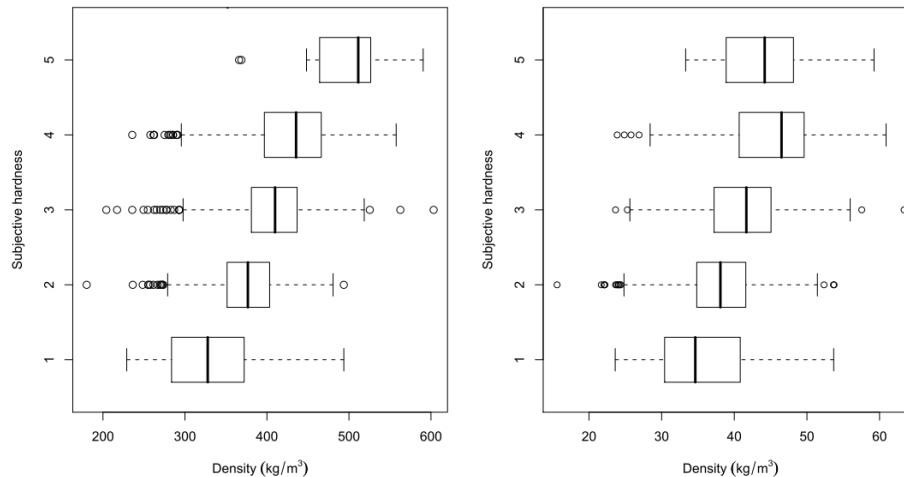
Fig. 12. Relationship between snow density and subjective hardness along the traverse sampled during summer 2003/04 (left) and 2004/05 (right). The hardness classes in the y-axis are fist (class 1), 4-fingers (class 2), 1-finger (class 3), pen (class 4), knife (class 5), and solid ice (class 6). The vertical line inside the box describes the median for the current class, the box extends from the 25% quartile to 75% quartile and the whiskers extend to 1.5 times the inter-quartile range. Outliers are shown as separate markers.
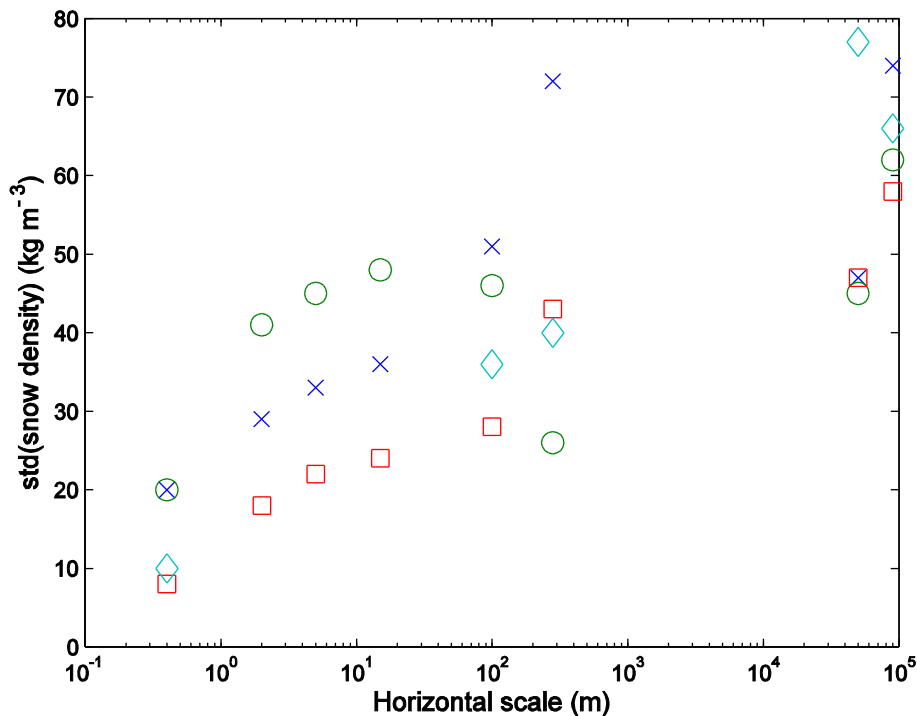
Fig. 13. Spatial standard deviation of snow density measured at various sampling scales. The results for the horizontal scale of 280 m are calculated on the basis of the data presented in Fig. 7 of Sturm and Benson (2004). The measurement depth is indicated by crosses for 0.02 m, circles for 0.1 m, squares for 0.2 m, and diamonds for 0.5 m.

Title Page

Abstract | Introduction

Conclusions | References

Tables | Figures

|◄ | ►|

◄ | ►

Back | Close

Full Screen / Esc

Printer-friendly Version

Interactive Discussion